Applied Catalysis A: General 494 (2015) 41–47

Contents lists available at ScienceDirect

Applied Catalysis A: General

journal homepage: www.elsevier.com/locate/apcata

Chemoselective hydrogenation of unsaturated nitriles to unsaturated primary amines: Conversion of cinnamonitrile on metal-supported catalysts

D.J. Segobia, A.F. Trasarti, C.R. Apesteguía *

Catalysis Science and Engineering Research Group (GICIC), INCAPE, UNL-CONICET, Santiago del Estero 2654, (3000) Santa Fe, Argentina

ARTICLE INFO

Article history:
Received 13 November 2014
Received in revised form 10 January 2015
Accepted 16 January 2015
Available online 28 January 2015

Keywords:
Cinnamonitrile hydrogenation
Unsaturated amines synthesis
Selective hydrogenation
Metal-supported catalysts

ABSTRACT

The liquid-phase hydrogenation of cinnamonitrile to selectively obtain the unsaturated primary amine (cinnamylamine) was studied at 383 K and 13 bar on Ni, Co, Ru and Cu metals supported on a commercial silica. Ni/SiO_2 and Co/SiO_2 were the most active catalysts for cinnamonitrile conversion but formed only small amounts of cinnamylamine. In contrast, Cu/SiO_2 and Ru/SiO_2 presented low activity for cinnamonitrile hydrogenation but formed selectively cinnamylamine in the liquid phase; nevertheless, on both samples the carbon balance was only about 40%. In an attempt of promoting the rate and yield to cinnamylamine, additional catalytic runs were carried out at higher temperatures and H_2 pressures on a highly dispersed $Cu(11\%)/SiO_2$ catalyst prepared by the chemisorption–hydrolysis method. Results showed that when cinnamonitrile hydrogenation was performed at 403 K and 40 bar on $Cu(11\%)/SiO_2$, the yield to cinnamylamine was 74% giving as by-product only the unsaturated secondary amine (dicinnamylamine).

1. Introduction

The liquid-phase selective hydrogenation of unsaturated nitriles on solid catalysts is an important route to obtain unsaturated primary amines that are valuable intermediates in agrochemical, pharmaceutical, and fine chemicals industries [1,2]. Nevertheless, the selective hydrogenation of the C≡N group in unsaturated nitriles is still a challenging objective in heterogeneous catalysis [3]. In general, the hydrogenation of unsaturated nitriles may form three types of products: unsaturated amines (hydrogenation of C≡N bond), saturated nitriles (hydrogenation of C=C bond) and saturated amines (hydrogenation of C=C and C≡N bonds). Besides, in order to obtain selectively primary amines the coupling reactions leading to secondary and tertiary amines have to be avoided. Previous works have reported that C=C bonds are more reactive to hydrogenation than the nitrile groups [4,5] and therefore selective C≡N hydrogenation in presence of double bonds is difficult to achieve, in particular when both unsaturated groups are conjugated or in close proximity [6]. Most of the few papers dealing with the hydrogenation of unsaturated nitriles on solid catalysts have been carried out on Ni and Co-based catalysts [4,5,7,8], probably because both metals are highly active and selective to obtain saturated primary amines from the corresponding saturated nitrile [9–11]. However, in the case of unsaturated nitriles, Raney Ni and Co catalysts promote the preferential hydrogenation to the corresponding saturated nitrile rather than to the unsaturated primary amine [3]. Thus, in an attempt of tuning the Ni(Co) selectivity to the formation of unsaturated primary amines, Cr-doped Raney Ni(Co) catalysts and amorphous Ni(Co)–B alloys were employed, but significant yields to the unsaturated amine where obtained only when alkaline or ammonia solutions were co-fed to the reactor [3,6,12]. Ammonia is often employed to suppress the formation of higher amines by shifting equilibrium to the primary amine since ammonia is released in the coupling reactions leading to secondary and tertiary amines; nevertheless, the addition of ammonia entails concerns related to corrosion and disposal of spent base materials.

Cinnamonitrile has been used as a substrate molecule to study the hydrogenation of α,β-unsaturated nitriles [3,6]. In this compound, the C=C bond is in conjugation with the nitrile as well as with the phenyl group. In Scheme 1 we present a possible reaction network of the cinnamonitrile conversion to primary and higher amines according to [3]. Cinnamonitrile (CN) may be initially hydrogenated in the C=C bond to yield hydrocinnamonitrile (HCN) or in the C≡N group producing cinnamylamine (CA), the desired unsaturated primary amine, probably via the formation of an imine intermediate (cinnamylimine). CA may then react with the

* Corresponding author. Tel.: +54 342 4555279; fax: +54 342 4531068.
E-mail addresses: capesteg@fiq.unl.edu.ar, capesteg@gmail.com (C.R. Apesteguía).
URL: http://www.fiq.unl.edu.ar/gicic/ (C.R. Apesteguía).

http://dx.doi.org/10.1016/j.apcata.2015.01.028
0926-860X/

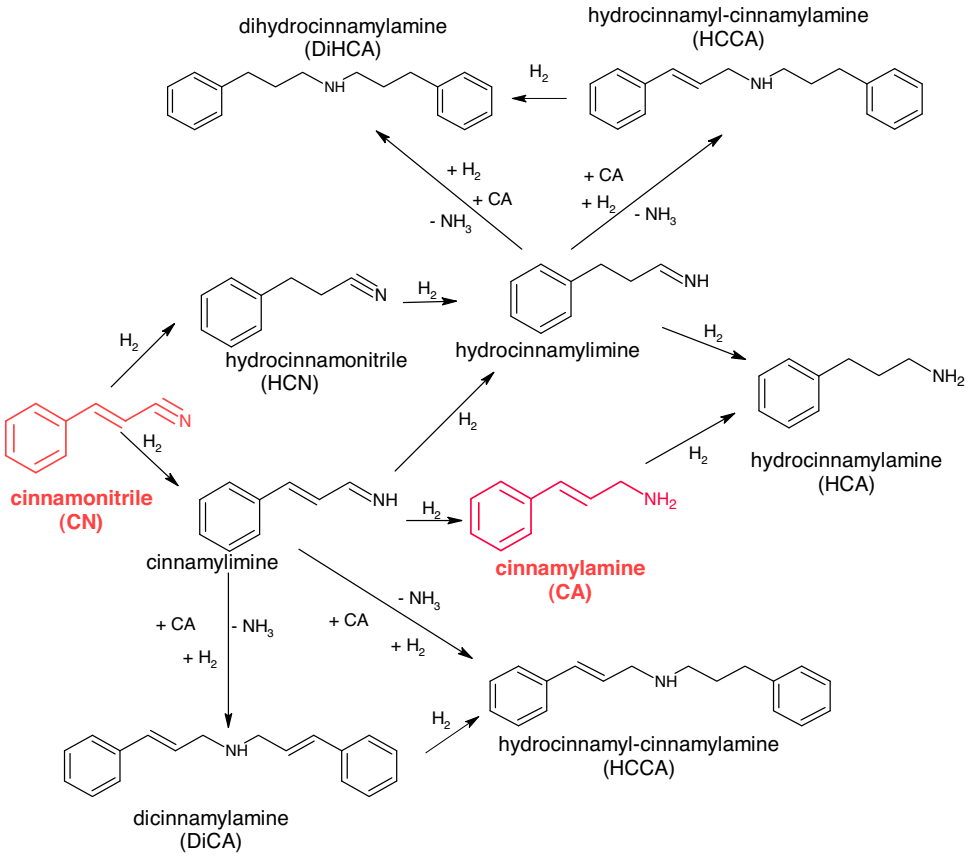

Scheme 1. Probable reaction network of cinnamonitrile conversion reactions

imine intermediate to form by deamination the unsaturated secondary amine dicinnamylamine (DiCA) and partially unsaturated secondary amine hydrocinnamyl-cinnamylamine (HCCA). Otherwise, CA may be hydrogenated to the saturated primary amine (hydrocinnamylamine, HCA). Similarly, in parallel pathways, HCN may be hydrogenated to HCA or it may react with the imine intermediate (hydrocinnamylimine) to produce by deamination the saturated secondary amine (dihydrocinnamylamine, DiHCA) and partially unsaturated secondary amine HCCA. According to bibliography, the highest yields to CA (≈70%) from cinnamonitrile hydrogenation have been obtained on Cr-doped Raney cobalt catalysts at 373 K, using 14% NH_3 in methanol and 80 bar H_2 [3].

In this work, we investigate the selective hydrogenation of cinnamonitrile to CA on silica-supported Co, Ni, Ru and Cu metals. In our catalytic tests, we detected and identified all the compounds depicted in Scheme 1, excepting the highly reactive imine intermediates. The goal of our work was twofold: (i) to establish the effect of the nature of the metal on the catalyst activity and selectivity for selectively obtaining CA from cinnamonitrile hydrogenation; (ii) to achieve high CA yields from cinnamonitrile conversion by selecting efficient metal-supported catalysts and optimizing reaction operating conditions, without using ammonia in the reaction media. Results will show that Cu/SiO_2 catalyst remarkably promotes the selective formation of CA from cinnamonitrile, thereby yielding 74% of CA at 403 K and 40 bar H_2, in absence of ammonia.

2. Experimental

2.1. Catalyst preparation

Co/SiO_2, Ni/SiO_2, Cu/SiO_2 and Ru/SiO_2 catalysts were prepared by supporting Co, Ni, Cu, or Ru on a SiO_2 powder (Sigma–Aldrich G62, 60–200 mesh, 300 m^2/g) by incipient-wetness impregnation at 303 K. Metal nitrate solutions [$Co(NO_3)_2{\cdot}6H_2O$ Aldrich 98%, $Ni(NO_3)_2{\cdot}6H_2O$ Fluka 98%, $Cu(NO_3)_2{\cdot}3H_2O$ Anedra 98%] were used for impregnating Co, Ni, and Cu while Ru/SiO_2 was prepared by using $RuCl_3{\cdot}H_2O$ (Aldrich 99.98%). The impregnated samples were dried overnight at 373 K, then heated in air at 5 K/min to 673 K and kept at this temperature for 2 h. Cu/SiO_2-I and Cu/SiO_2-II catalysts were obtained by supporting Cu on Grace Davison Davisil (grade 634, 320 m^2/g) and Merck (chromatographic, 366 m^2/g) silicas, respectively, using the chemisorption–hydrolysis method as detailed elsewhere [13]. The support was added to a solution containing $[Cu(NH_3)_4]^{2+}$ and the slurry was slowly diluted with water. Then, solids were separated by filtration, washed with water, dried overnight at 383 K and calcined in air at 623 K for 4 h.

2.2. Catalyst characterization

BET surface areas (S_g) were measured by N_2 physisorption at its boiling point in a Micromeritics Accusorb 2100E sorptometer. Elemental compositions were measured by inductively coupled plasma atomic emission spectroscopy (ICP-AES), using a Perkin-Elmer Optima 2100 unit. Powder X-ray diffraction (XRD) patterns were collected in the range of $2\theta = 10–70^\circ$ using a Shimadzu XD-D1 diffractometer and Ni-filtered Cu Kα radiation. Oxide crystallite sizes were calculated using the Debye–Scherrer equation.

The temperature programmed reduction (TPR) experiments were performed in a Micromeritics AutoChem II 2920, using 5% H_2/Ar gaseous mixture at 60 cm^3/min STP. The sample size was 150 mg. Samples were heated from 298 to 973 K at 10 K/min.

The metal dispersions (D_M, surface M atoms/total M atoms) of Ni/SiO_2 and Ru/SiO_2 were determined by H_2 chemisorption. Volumetric adsorption experiments were performed at 298 K in

a conventional vacuum unit. Catalysts were reduced in H_2 at 673 K for 2 h and then outgassed 2 h at 673 K prior to performing gas chemisorption experiments. Hydrogen uptake was determined using the double isotherm method [14]. A stoichiometric atomic ratio of $H/M_s = 1$, where M_s implies a metal atom on surface, were used to calculate the metal dispersion. The copper dispersion was measured by combining N_2O oxidation with TPR, according to Sato et al. [15]. Cu-containing samples were reduced in H_2(5%)/Ar for 1 h at 623 K and then exposed to pulses of N_2O at 363 K in a flow of He. The evolution of the N_2O signal ($m/z = 44$) was followed by mass spectrometry in a Balzers Omnistar spectrometer. When the N_2O signal intensity was constant indicating that the Cu surface oxidation was completed, the system was purged in Ar and then a TPR run was carried out using a H_2(5%)/Ar flow (60 cm^3/min) and by increasing the temperature from 363 K to 623 K at 10 K/min. The H_2 consumption was monitored by mass spectrometry; quantitative H_2 uptakes were calculated by integration of the experimental TPR curves and the number of chemisorbed oxygen atoms was calculated by using a $Cu_s/N_2O = 2$ stoichiometry [16].

2.3. Catalytic activity

Standard catalytic runs for the liquid-phase hydrogenation of cinnamonitrile (Aldrich, >98%) were carried out at 383 K and 13 bar (H_2) in a Parr 4843 batch reactor. The autoclave was loaded with 150 mL of solvent (toluene, Cicarelli, ACS), 1.5 mL of cinnamonitrile, 0.5 g of catalyst, and 1 mL of n-hexadecane (Aldrich >99%) as internal standard. Prior to catalytic tests, samples were reduced ex-situ in hydrogen (60 mL/min) for 2 h at 543 K (Cu) or 673 K (Co, Ni, Ru) and loaded immediately to the reactor at room temperature under inert atmosphere. The reaction system was stirred at 800 rpm and heated to the reaction temperature at 2 K/min; the H_2 pressure was then rapidly increased to 13 bar. Product concentrations were followed during the reaction by ex-situ gas chromatography using an Agilent 6850 GC chromatograph equipped with flame ionization detector, temperature programmer and a 50 m HP-1 capillary column (50 m × 0.32 mm ID, 1.05 μm film). Product identification was achieved using a Varian Saturn 2000 GC–MS unit with a VF5ht capillary column. Samples from the reaction system were taken by using a loop under pressure in order to avoid flashing. Data were collected every 15–40 min for 300–600 min. The main reaction products detected were saturated nitrile HCN, unsaturated primary amine CA, saturated primary amine HCA, unsaturated secondary amine DiCA, partially unsaturated secondary amine HCCA and saturated secondary amine DiHCA. The presence of tertiary amines was not detected in any case. The batch reactor was assumed to be perfectly mixed. Interparticle and intraparticle diffusional limitations were verified as negligible. Conversion of cinnamonitrile was calculated as $X_{CN} = (C^0_{CN} - C_{CN})/C^0_{CN}$, where C^0_{CN} is the initial concentration of cinnamonitrile and C_{CN} is the concentration of cinnamonitrile at reaction time t. Selectivities (S_j, mol of product j/mol of cinnamonitrile reacted) were calculated as $S_j = C_j\nu_{CN}/(C^0_{CN} - C_{CN})\nu_j$ where ν_{CN} and ν_j are the stoichiometric coefficients of cinnamonitrile and product j, respectively. Yields (η_j, mol of product j/mol of cinnamonitrile fed) were calculated as $\eta_j = S_j X_{CN}$.

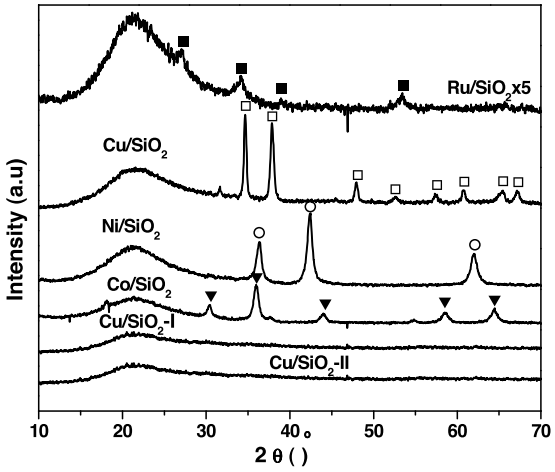

Fig. 1. X-ray diffractograms of calcined samples. ■ RuO_2, □ CuO, ○ NiO, ▼ Co_3O_4

3. Results and discussion

3.1. Catalyst characterization

The metal loadings and physical properties of the catalysts are presented in Table 1. The surface area of the three different silicas used as support did not change significantly after the metal impregnation and the consecutive oxidation/reduction steps used for obtaining metal/SiO_2 catalysts. The XRD patterns of calcined samples are shown in Fig. 1. RuO_2 (ASTM 21-1172), CuO (ASTM 5-0661), NiO (ASTM 4-835) and Co_3O_4 (ASTM 9-418) were identified on Ru/SiO_2, Cu/SiO_2, Ni/SiO_2 and Co/SiO_2, respectively. In contrast, the XRD diffractograms of Cu/SiO_2-I and Cu/SiO_2-II did not show the presence of crystalline metal oxides. The oxide particle sizes determined using the Debye–Scherrer equation were 18 nm (CuO), 12 nm (NiO) and 12 nm (Co_3O_4). The XRD signal obtained for RuO_2 on Ru/SiO_2 was too weak for determining with exactitude the RuO_2 particle size.

The sample TPR profiles are shown in Fig. 2 and the corresponding temperature maxima (T_{max}) are included in Table 1. The Ni/SiO_2 TPR curve exhibited a broad reduction band with a maximum at 643 K corresponding to the direct reduction of NiO to metallic nickel. No reduction peak at higher temperatures that would reveal the presence of less reducible surface Ni silicates was observed. The TPR profile of Co/SiO_2 showed two reduction peaks at 573 K and 623 K, respectively, which result from the reduction of Co_3O_4 following the sequence $Co^{3+} \rightarrow Co^{2+} \rightarrow Co^0$ [17,18]. Reduction of CuO on Cu/SiO_2 gave rise to a broad H_2 consumption

Table 1
Catalyst characterization.

Catalyst	Metal loading[a] (%)	S_g (m^2/g)	Metal dispersion D_M (%)	Oxide particle size[d] (nm)	TPR, T_{max} (K)
Co/SiO_2	9.8	307	–	12 (Co_3O_4)	573, 623
Ni/SiO_2	10.5	290	1[b]	12 (NiO)	643
Ru/SiO_2	1.8	280	2[b]	n.d.	470
Cu/SiO_2	9.2	285	1[c]	18 (CuO)	543
Cu/SiO_2-I	7.6	321	32[c]	n.d.	497
Cu/SiO_2-II	11.0	386	21[c]	n.d.	507

n.d.: not detected.
[a] Determined by ICP-AES.
[b] Determined by H_2 chemisorption.
[c] Determined by N_2O titration.
[d] Determined from the XRD diffractogram using the Debye–Scherrer equation.

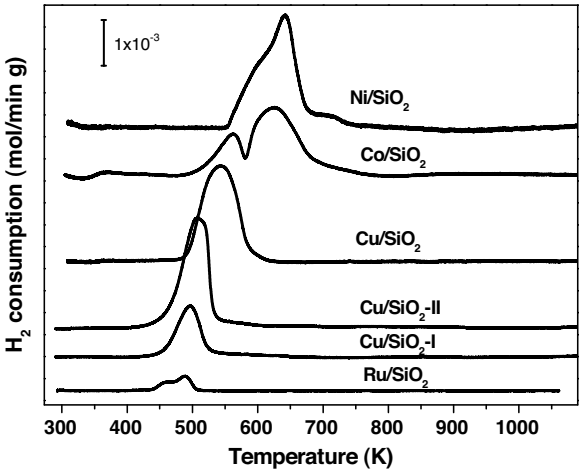

Fig. 2. TPR profiles of the samples used in this work

band, which suggests a heterogeneous size distribution of the CuO particles [19]. The temperature maximum for CuO reduction on Cu/SiO_2 (543 K) was higher than on Cu/SiO_2-I (497 K) and Cu/SiO_2-II (507 K), probably reflecting that Cu/SiO_2 contains bigger CuO crystallites according to XRD characterization data in Fig. 1. The increase of T_{max} with the CuO crystallite size is consistent with the unreacted shrinking core model predictions for non-porous metal oxides reduction. Previous works [20,21] have effectively furnished convincing experimental evidence for the dependence of T_{max} on particle size by modeling TPR profiles of different-sized particles of CuO with the unreacted core model. Taking into account the T_{max} values in Table 1, it is inferred that on all the catalysts used in this work the metal fraction is totally in the metallic state following the standard reduction step used prior to catalytic tests (reduction in pure H_2 at 543 K for Cu/SiO_2 and at 673 K for the rest of metal/SiO_2 samples). Finally, the Ru/SiO_2 TPR curve exhibited two superimposed reduction peaks that probably reflect the existence of a bimodal distribution of particle sizes, as reported in bibliography for Ru-supported catalysts obtained by calcination of $RuCl_3$ precursors [22].

The obtained metal dispersion values are also presented in Table 1. The metallic dispersion of Ni on Ni/SiO_2 was only about 1% and this result is consistent with the large NiO crystallite sizes determined from the X-ray diffraction pattern of Fig. 1. This low D_{Ni} value is consequence of both the high Ni loading, and the preparation method used to impregnate Ni nitrates onto silica. Ru dispersion on Ru/SiO_2 catalyst was also low, about 2%. The D_{Cu} value determined on Cu/SiO_2 catalyst was only 1%, which is consistent with the large CuO crystallite size determined by XRD and probably reflects a weak interaction between the copper crystallites and the support. In contrast, the Cu dispersion was high on Cu/SiO_2-I (32%) and Cu/SiO_2-II (21%), thereby confirming that preparation of Cu-supported catalysts by the chemisorption–hydrolysis method leads to the formation of small Cu particles [13,23].

3.2. Catalyst activity and selectivity

In Fig. 3 we have represented the CN conversion and yields as a function of parameter $W \cdot t/n^0_{CN}$, where t is the reaction time, W is the catalyst weight, and n^0_{CN} the initial moles of cinnamonitrile. The local slope of each curve in Fig. 3 gives the CN conversion rate at a specific value of CN conversion and reaction time. The initial CN conversion rate per g of metal (r^0_{CN}, mmol/h g_M) determined from the curves of Fig. 3 is shown in Table 2. The values of X_{CN} and selectivities S_i at the end of the runs are also presented in Table 2. Data in Table 2 show that r^0_{CN} followed the order: Ni > Co > Ru > Cu. On Ni/SiO_2 and Co/SiO_2, X_{CN} rapidly increased with the progress of the reaction reaching 100% at the end of the runs. In contrast,

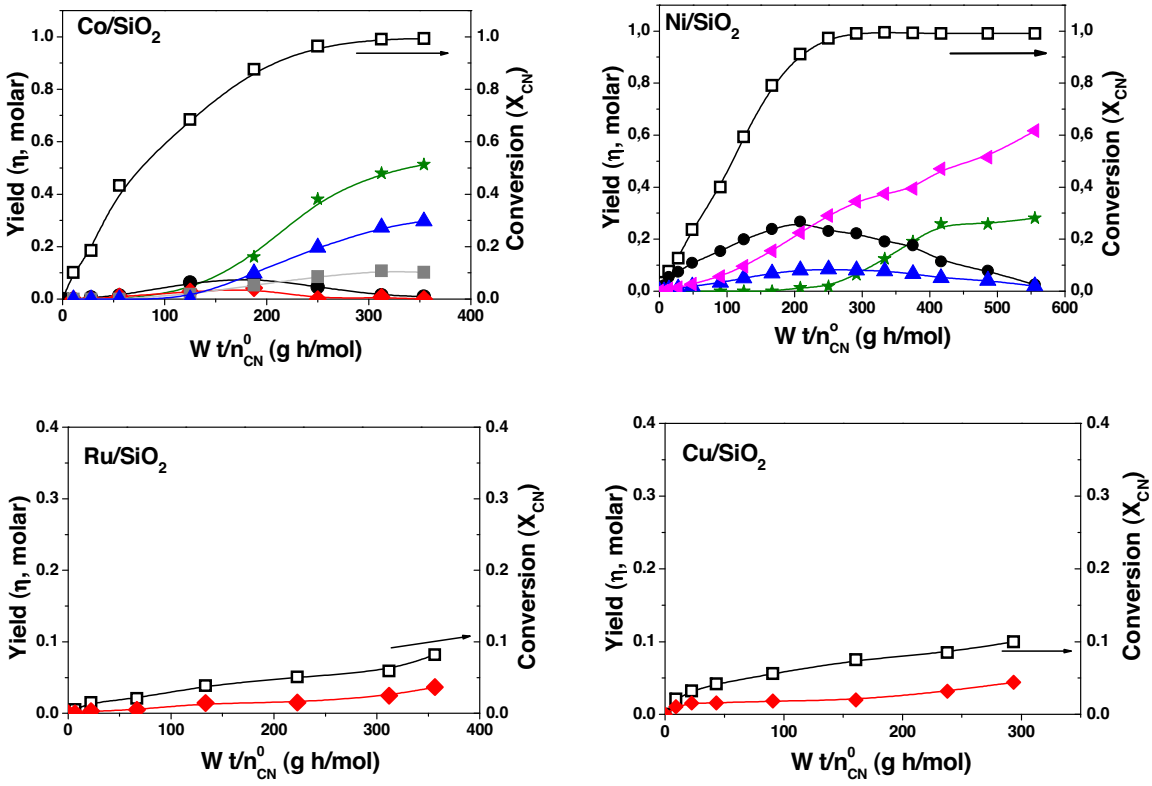

Fig. 3. Catalytic results: cinnamonitrile conversion (X_{BN}) and yields (η_i). ● HCN, ★ HCA, ▲ HCCA, ◆ CA, ◀ DiHCA, ■ DiCA [T = 383 K, P = 13 bar, W_{cat} = 0.5 g].

Table 2
Catalytic results.

Catalyst	Reaction length (min)	Initial activity	Conversion (X_{CN},%) and selectivities (%) at the end of reaction						
		r^0_{CN} (mmol/h g_M)	X_{CN}	CA	HCA	DiCA	DiHCA	HCAA	Others
Co/SiO_2	500	90	100	–	52	10	–	30	8
Ni/SiO_2	800	102	100	–	33	–	63	–	4
Ru/SiO_2	500	33	8	40	–	–	–	–	60
Cu/SiO_2	430	23	10	46	–	–	–	–	54

T = 383 K, r^0_{CN} = 13 bar, W_{cat} = 0.5 g, V_{CN} = 1.5 mL, solvent: toluene (150 mL).

the CN conversion on Ru/SiO_2 and Cu/SiO_2 slowly increased with reaction time reaching only about 10% after 360 min of reaction.

Regarding catalyst selectivity, Fig. 3 shows that CN was rapidly converted on Co/SiO_2 but formation of primary products HCN and CA was detected only after a long induction period of about 100 min, probably reflecting a strong adsorption of the reactant and intermediates. HCN and CA reached a maximum yield as they converted to saturated primary amine HCA and secondary amines, HCCA and DiCA, with increasing reaction time (Scheme 2A). At the end of the run, Co/SiO_2 yielded 52% of HCA and the carbon balance was 92% (Table 2). Initially, Ni/SiO_2 selectively hydrogenated CN to HCN and we did not detect unsaturated primary amine CA among the reaction products. Then, the HCN yield curve in Fig. 3 went through a maximum because HCN was converted to saturated primary amine HCA and to secondary amines HCCA and DiHCA. Unsaturated secondary amine HCCA was completely hydrogenated to DiHCA with the progress of the reaction so that at the end of the catalytic test the product mixture contained only DiHCA (63%) and HCA (33%). Scheme 2B summarizes the consecutive reaction pathways leading from CN to final products on Ni/SiO_2 catalyst. Finally, on Ru/SiO_2 and Cu/SiO_2 we observed the formation of only one product: unsaturated primary amine CA. However, CN conversion did not exceed 10% on both catalysts revealing the sample deactivation with the progress of the reaction, probably because of a strong adsorption of reactant, intermediate and products on the metals since the carbon balance was very low on these catalysts (40–46%, Table 2).

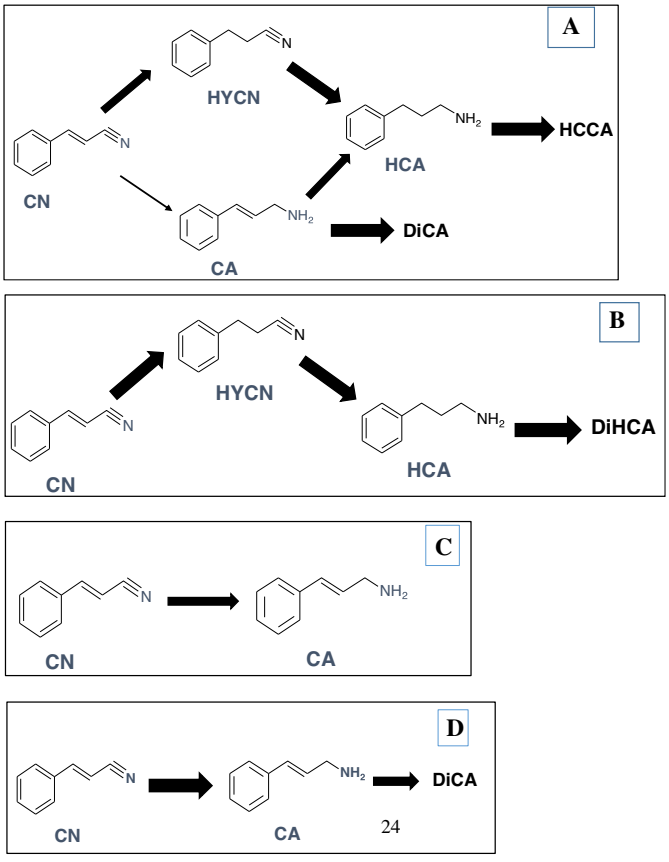

Scheme 2. Main reaction pathways for cinnamonitrile conversion reactions on: (A) Co/SiO_2, (B) Ni/SiO_2, (C) Cu/SiO_2 or Ru/SiO_2, (D) Cu/SiO_2-II. The line width indicates the relative relevance of each reaction.

The different catalytic performances of the samples in Table 2 may be interpreted by considering the ratio of repulsive and attractive forces (F_R/F_A) existing between the emergent d-orbitals of the metal and the adsorbate, as frequently observed in bibliography for hydrogenation reactions involving α,β-unsaturated compounds [24–26]. In a simple way, the relative intensity of F_R and F_A forces is usually related to the combination of extent and filling of the metal d bands. The order of d-orbital filling for the non-noble metals used in this work is Co < Ni < Cu, while the d-band extent follows the opposite order Cu < Ni < Co. In our case, the repulsive forces existing between metal d-orbitals and the phenyl group of CN molecule would increase with the filling of d-orbitals. It can be expected therefore that a low interaction between the CN phenyl group and the metallic Cu surface takes place because in Cu^0 the d-orbitals are completely filled (Fig. 4). The CN adsorption on Cu would occur then mainly via its C≡N group, thereby favoring the formation of nitrene intermediates (i.e. formation of N═Cu bonds) which would lead to the preferential hydrogenation of CN to unsaturated amine CA. Previous works have reported, in fact, that the nitrene intermediates promotes the selective formation of primary amines at the expense of the parallel condensation to secondary amines [27,28]. In the case of Ni, the F_R/F_A ratio for CN adsorption is lower as compared to Cu because the d-band of Ni is only partially filled. Consequently, the interaction between the substrate and Ni probably occurs via the C═C group of the CN molecule which would promote the selective CN hydrogenation to HCN, as we observed in Fig. 3. Finally, it is expected a weak interaction between the CN phenyl group and cobalt because this metal presents the largest d-orbital extent (Fig. 4). This would favor the CN adsorption on Co through its C≡N group which turns more accessible the C═C group of CN to the metal surface and allows its rapid hydrogenation to saturated amine HC. Besides, it has been reported that formation of carbenes from the C≡N group adsorption leads also to the production of secondary amines [27,29].

In summary, Ni/SiO_2 and Co/SiO_2 were the most active catalysts for CN conversion but formed only small amounts of unsaturated primary amine CA. Ni/SiO_2 yielded a mixture of saturated primary (HCA) and secondary (DiHCA) amines while Co/SiO_2 produced a mixture of saturated primary amine HCA, unsaturated secondary amine DiCA, and partially unsaturated secondary amine HCCA. In contrast, Cu/SiO_2 and Ru/SiO_2 presented low activity for CN hydrogenation at 383 K but formed selectively unsaturated amine CA in the liquid phase; nevertheless, on both samples the carbon balance was only about 40%. Taking into account that our goal was to efficiently produce unsaturated primary amine CA via CN hydrogenation, we decided to perform additional catalytic runs using more dispersed Cu/SiO_2 catalysts at higher reaction temperatures in order to substantially increase the catalyst activity. We selected Cu instead of Ru to perform this study because previous work

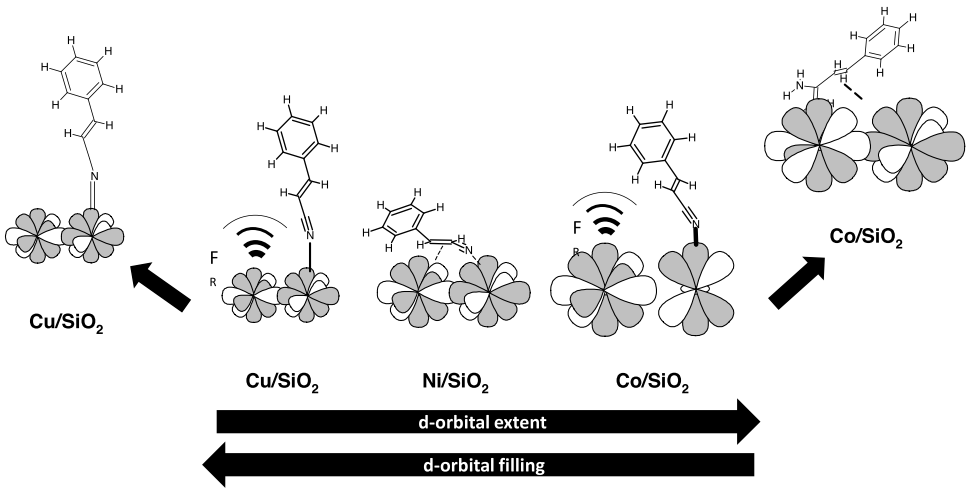

Fig. 4. Schematic representation of the interaction between the cinnamonitrile molecule and the transition metal surface

Table 3
Catalytic results on Cu catalysts.

Catalyst	Temperature (K)	Pressure (bar)	Reaction length (min)	Initial activity r^0_{CN} (mmol/h g_{Cu})	Conversion (X_{CN}, %) and selectivities (%)[a]			
					X_{CN}	CA	DiCA	Others
Cu/SiO_2-I	383	13	540	39	19	52	–	48
Cu/SiO_2-II	383	13	560	75	40	59	11	30
Cu/SiO_2-II	403	13	1170	201	96	60	28	12
Cu/SiO_2-II	403	25	650	359	98	67	23	10
Cu/SiO_2-II	403	40	600	580	100	74	20	6

W_{cat} = 0.5 g, V_{CN} = 1.5 mL, solvent: toluene (150 mL).
[a] Determined at the end of the reaction.

[30,31] showed that Cu exhibits poor activity for hydrogenating isolated C=C bonds of α,β-unsaturated compounds, which is a desirable metal property in our case for selectively obtaining unsaturated primary amines from unsaturated nitriles hydrogenation.

3.3. Selective synthesis of CA on silica-supported Cu catalysts

Additional catalytic runs for CN hydrogenation were carried out on Cu/SiO_2-I and Cu/SiO_2-II catalysts. Results obtained at 383 K and 13 bar are given in Table 3 (two first rows). The initial CN conversion rates determined on Cu/SiO_2-I (r^0_{CN} =39 mmol/h g_{Cu}) and Cu/SiO_2-II (r^0_{CN} = 75 mmol/h g_{Cu}) were higher than that obtained on Cu/SiO_2 (r^0_{CN} = 23 mmol/h g_{Cu}) at similar reaction conditions. Consistently, the X_{CN} conversion at the end of the runs increased from 10% (Cu/SiO_2) to 19% (Cu/SiO_2-I) and 40% (Cu/SiO_2-II). The final selectivity to CA also increased from 46% (Cu/SiO_2) to 52% (Cu/SiO_2-I) and 59% (Cu/SiO_2-II). Formation of unsaturated secondary amine DiCA was observed on Cu/SiO_2-II (S_{DiCA} = 11%) but not on Cu/SiO_2-I. On the other hand, the carbon balance at the end of the runs improved from 46% (Cu/SiO_2) to 52% (Cu/SiO_2-I) and 70% (Cu/SiO_2-II). All these results showed that the catalyst activity, selectivity, and stability for CA formation were clearly improved when the Cu dispersion was increased.

In an attempt of promoting further the rate and yield to CA, we performed catalytic tests on Cu/SiO_2-II (the most active and selective catalyst) at higher temperatures and H_2 pressures. Results obtained at 403 K and 13 bar are presented in Table 3 (third row). As expected, the initial CN conversion rate increased with temperature, from 75 mmol/h g_{Cu} (383 K) to 201 mmol/h g_{Cu} (430 K) and X_{CN} reached 96% at the end of the run. As a consequence, the yield to CA on Cu/SiO_2-II increased from 23.6% (383 K) to 57.6% (430 K), in spite that the CA selectivity did not change with the increase of temperature. Significant amounts of DiCA were obtained on Cu/SiO_2-II at 403 K, reaching S_{DiCA} a value of 28% at the end of the run. These later results show that at 403 K CN is converted on Cu/SiO_2-II via a single reaction pathway involving the initial CN hydrogenation to unsaturated primary amine CA that forms consecutively the unsaturated secondary amine DiCA (Scheme 2D). We confirm then that Cu does not form saturated amines from CN because is inactive for hydrogenating isolated C=C bonds. The global carbon balance also improved with temperature, from 70% (383 K) to 88% (430 K).

Finally, we investigated the effect of increasing the H_2 pressure from 13 bar to 25 bar and 40 bar on the catalytic performance of Cu/SiO_2-II catalyst at 403 K. Fig. 5 illustrates the evolution of CN conversion and yields as a function of time obtained on Cu/SiO_2-II at 40 bar. Results in Table 3 show that r^0_{CN} increased almost proportionally with P_{H_2} indicating that the reaction order with respect to hydrogen was about one. Complete CN conversion was obtained at the end of the 600-min run performed at 40 bar (Fig. 5). The final selectivity to CA increased from 60% (13 bar) to 74%

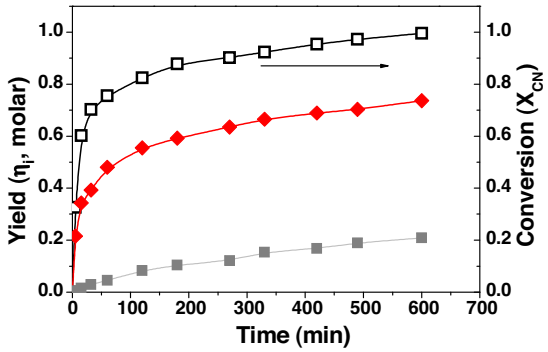

Fig. 5. Cinnamonitrile conversion (X_{BN}) and yields (η_i) on Cu/SiO_2-II catalyst ◆ CA, ■ DiCA [T = 403 K, P = 40 bar, W_{cat} = 0.5 g].

(40 bar) while S_{DiCA} decreased from 28% to 20%; i.e., the increase of H_2 pressure enhanced the CN hydrogenation to CA at the expense of the competitive condensation reaction leading to secondary amine DiCA (Scheme 1). The carbon balance also improved with P_{H_2}, from 88% (13 bar) to 94% (40 bar). In summary, Cu/SiO_2-II prepared by chemisorption–hydrolysis is an efficient catalyst for promoting the selective hydrogenation of cinnamonitrile to the unsaturated primary amine because combines a significant activity for BN conversion (it contains a high amount of well dispersed copper) with the ability of Cu for selectively hydrogenating the CN group of cinnamonitrile. Thus, our results show that Cu/SiO_2-II yields 74% of CA at 403 K and 40 bar H_2, without the presence of ammonia.

4. Conclusions

The activity and selectivity of silica-supported Ni, Co, Ru and Cu catalysts for hydrogenating cinnamonitrile to cinnamylamine greatly depend on the nature of the metal and reaction operating conditions. At 383 K and 13 bar H_2, Ni/SiO_2 is a very active catalyst that promotes the preferential hydrogenation of C=C bonds thereby forming mainly saturated nitriles and amines. Co/SiO_2 is also a very active catalyst, but produces initially only small amounts of cinnamylamine that are rapidly converted to saturated primary and secondary amines. In contrast, Ru/SiO_2 and Cu/SiO_2 catalysts are significantly less active than Ni/SiO_2 or Co/SiO_2 and deactivate during the progress of the reaction; however, both catalysts form mainly cinnamylamine. The Cu/SiO_2 activity, selectivity and stability for the production of cinnamylamine may be remarkably enhanced by improving the Cu dispersion and increasing the reactor temperature and pressure. In fact, we report here that at 403 K and 40 bar, the $Cu(9.2\%)/SiO_2$ catalyst prepared by the chemisorption–hydrolysis method yields 74% of cinnamylamine from cinnamonitrile hydrogenation without the addition of any secondary amine formation suppressant such as ammonia, and gives as by-product only the unsaturated secondary amine.

Acknowledgements

Authors thank the Universidad Nacional del Litoral (UNL), Consejo Nacional de Investigaciones Cientificas y Tecnicas (CONICET), and Agencia Nacional de Promocion Cientifica y Tecnologica (ANPCyT), Argentina, for the financial support of this work.

References

[1] G. Petranyi, N.S. Ryder, A. Stutz, Science 224 (1984) 1239–1241.
[2] I. Minamida, K. Iwanaga, T. Okauchi, Takeda Chemical Industries, Ltd., US 6,407,248 (2002).
[3] P. Kukula, M. Studer, H.-U. Blaser, Adv. Synth. Catal. 346 (2004) 1487–1493.
[4] J.L. Dallons, G. James, B. Delmon, Catal. Today 5 (1989) 257–264.
[5] A.S. Canning, S.D. Jackson, S. Mitchell, Catal. Today 114 (2006) 372–376.
[6] P. Kukula, K. Koprivova, J. Catal. 234 (2005) 161–171.
[7] T. Tihani, K. Varga, I. Hannus, I. Kiricsi, P. Fejes, React. Kinet. Catal. Lett. 18 (1981) 449–454.
[8] P. Kukula, V. Gabova, K. Koprivova, P. Trti, Catal. Today 121 (2007) 27–38.
[9] A. Chojecki, M. Veprek-Heijman, T.E. Muller, P. Scharringer, S. Veprek, J.A. Lercher, J. Catal. 245 (2007) 237–248.
[10] D.J. Segobia, A.F. Trasarti, C.R. Apesteguía, Appl. Catal. A: Gen. (2012) 445–446.
[11] D.J. Segobia, A.F. Trasarti, C.R. Apesteguía, J. Braz. Chem. Soc. 25 (12) (2014) 2272–2279.
[12] C. Barnett, Ind. Eng. Chem. Prod. Res. Dev. 8 (1969) 145–149.
[13] F. Boccuzzi, A. Chiorino, G. Martra, M. Gargano, N. Ravasio, B. Carrozzini, J. Catal. 165 (1997) 129–139.
[14] A. Borgna, T.F. Garetto, C.R. Apesteguía, F. Le Normand, B. Moraweck, J. Catal. 186 (1999) 433–441.
[15] S. Sato, R. Takahashi, T. Sodesawa, K. Yuma, Y. Obata, J. Catal. 196 (2000) 195–199.
[16] A. Dandekar, M.A. Vannice, J. Catal. 178 (1998) 621–639.
[17] P. Grandvallet, P. Courty, E. Freund, A. Sugier, Proceedings of the 8th International Congress on Catalysis, Berlin 1984, vol. II, Ottawa, 1984, pp. 92–99.
[18] A.J. Marchi, J.I. Di Cosimo, C.R. Apesteguía, Catal. Today 15 (1992) 383–394.
[19] A.J. Marchi, D.A. Gordo, A.F. Trasarti, C.R. Apesteguía, Appl. Catal. A: Gen. 249 (2003) 53–67.
[20] K.H. Tonge, Thermochim. Acta 74 (1984) 151–166.
[21] M.J.L. Ginés, C.R. Apesteguía, Latinam. Appl. Res. 25 (1995) 215–221.
[22] D.E. Damiani, E.D. Pérez Millán, A.J. Rouco, J. Catal. 101 (1986) 162–168.
[23] A.F. Trasarti, D.J. Segobia, C.R. Apesteguía, F. Santoro, F. Zaccheria, N. Ravasio, J. Am. Oil Chem. Soc. 89 (2012) 2245–2252.
[24] F. Delbecq, P. Sautet, Catal. Lett. 28 (1994) 89–98.
[25] F. Delbecq, P. Sautet, J. Catal. 152 (1995) 217–236.
[26] N.M. Bertero, C.R. Apesteguía, A.J. Marchi, Appl. Catal. A: Gen. 349 (2008) 100–109.
[27] J. Krupka, J. Pasek, Curr. Org. Chem. 16 (2012) 988.
[28] D.J. Segobia, A.F. Trasart, C.R. Apesteguía, Catal. Sci. Technol. 4 (2014) 4075–4083.
[29] P. Scharringer, T.E. Muller, A. Jentys, J.A. Lercher, J. Catal. 263 (2009) 34.
[30] N. Ravasio, M. Antenori, M. Gargano, J. Mol. Catal. 74 (1992) 267–274.
[31] A.F. Trasarti, A.J. Marchi, C.R. Apesteguía, J. Catal. 247 (2007) 155–165.